

# Twofold Structured Features-Based Siamese Network for Infrared Target Tracking

Weijie Yan, Minjie Wan, Yunkai Xu, Xiaofang Kong, Ajun Shao, Qian Chen, and Guohua Gu

**Abstract**—Nowadays, infrared target tracking has been a critical technology in the field of computer vision and has many applications, such as urban security, pedestrian counting, smoke and fire detection, and so forth. Unfortunately, due to the lack of color, texture and other detailed information, tracking drift often occurs when the tracker encounters infrared targets that vary in size or shape. To address this issue, we present a twofold structured features-based Siamese network for infrared target tracking. First of all, in order to improve the discriminative capacity for infrared targets, a novel feature fusion network is proposed to fuse both shallow spatial information and deep semantic information into the extracted features in a comprehensive manner. Then, a multi-template update module is designed to effectively deal with interferences from target appearance changes which are prone to cause early tracking failures. Finally, both qualitative and quantitative experiments are carried out on VOT-TIR 2016 dataset, which demonstrates that our method achieves the balance of promising tracking performance and real-time tracking speed against other out-of-the-art trackers.

**Index Terms**—Twofold structured features, multi-template update, shallow spatial features, deep semantic features, Siamese network, infrared target tracking.

## I. INTRODUCTION

OWING to the rapid development of artificial intelligence nowadays, infrared target tracking has become one of the frontier issues in the field of computer vision and shows promising potential for many computational social system-related tasks [1] [2] [3], e.g., urban security [4], pedestrian counting [5], smoke and fire detection [6], and so forth. Meanwhile, as the infrared thermal imaging technology keeps advancing, infrared target tracking, which fits to work under various complex illumination conditions, has been deeply investigated for the past few decades. In this paper, we are dedicated to designing an infrared target tracker that is flexibly adaptable to different scenes.

This work was supported jointly by National Natural Science Foundation of China (62001234, 62201260), Natural Science Foundation of Jiangsu Province (BK20200487), the Equipment Pre-research Weapon Industry Application Innovation Project under Grant (627010402), the Equipment Pre-research Key Laboratory Fund Project under Grant (6142604210501). (Corresponding author: Minjie Wan.)

Weijie Yan, Minjie Wan, Yunkai Xu, Ajun Shao, Qian Chen, and Guohua Gu are with the School of Electronic and Optical Engineering, Nanjing University of Science and Technology, Nanjing 210094, China, and also with the Jiangsu Key Laboratory of Spectral Imaging & Intelligent Sense, Nanjing University of Science and Technology, Nanjing 210094, China. (email: yan-weijie@njjust.edu.cn; minjiewan1992@njjust.edu.cn; xuyunkai@njjust.edu.cn; njjustaj@njjust.edu.cn; chenq@njjust.edu.cn; gghnjjust@mail.njjust.edu.cn.) Xiaofang Kong is with National Key Laboratory of Transient Physics, Nanjing University of Science and Technology, Nanjing 210094, China. (e-mail: xiaofangkong@njjust.edu.cn).

Compared with visible light images, however, infrared images have their own particular limitations that lead to the degradation of tracking performance. First of all, due to the poor imaging quality of traditional infrared cameras, infrared images not only lack color, texture and many other details, but also suffer from low signal-to-noise ratio and image resolution, which makes it difficult for the tracker to distinguish the target from the background. Furthermore, infrared image is a kind of gray-scale image and is vulnerable to the surrounding environment, resulting in a wide range of changes in gray-scale distribution, contour shape, and other appearance information of the target [7]. In brief, it is more challenging to robustly track object of interests in infrared images than in visible light images.

Because of the promising accuracy and robustness, Siamese network-based trackers have been regarded as one of the most popular branches in the field of visual object tracking. Despite the advantages in handling visible light images, their tracking performance is rarely satisfactory when directly applied to treat infrared images. Bertinetto et al. [8] introduced an end-to-end training-based Siamese network into the field of target tracking for the first time, which improved the accuracy greatly by casting the tracking problem as measuring the similarity between input features. Since then, various target tracking methods based on Siamese networks have emerged. Li et al. [9] replaced the shallow backbone network by a modern depth network called ResNet, which makes a further step in extracting specific and comprehensive target features and however also brought certain problems. Specifically speaking, target features extracted by modern depth network always have the tendency of focusing too much on deep semantic information and thereby unconsciously ignoring shallow spatial information that is equally critical to infrared target tracking [10]. In addition, due to using fixed templates or simple linear variable templates, Siamese network-based trackers have poor adaptability to the apparent change of target which often occurs in infrared image [11]. Influenced by the two factors cited above, tracking drift is easy to happen when it comes to actual infrared scenes.

In this article, we propose a twofold structured features-based Siamese tracker equipped with the multi-template update module, named TSF-SiamMU, to overcome the two above-mentioned drawbacks of conventional depth network-based Siamese trackers when handling infrared images. First of all, a new feature fusion network which separately fuses shallow spatial information and deep semantic information into the extracted features is designed so as to greatly enhance the network's capacity in distinguishing the fuzzy infrared

target from the background. Further, we develop a template update mechanism which aims to estimate the current optimal template through the aggregation of the initial template, the accumulated template and the current template based on the previous prediction. Finally, in order to deal with various infrared target changes, a multi-template update module based on the template update mechanism is proposed, where differentiated update operations are applied to templates in diverse depth. Both qualitative and quantitative experiments implemented on real infrared sequences show that our method achieves real-time performance and is better than other state-of-the-art methods in terms of success rate and precision. In conclusion, the main contributions of this article can be summarized threefold as follows:

(1) A novel feature fusion network which separately fuses shallow spatial information and deep semantic information into the extracted features is proposed to improve the capacity of feature representation of infrared targets in a comprehensive manner.

(2) A multi-template update module based on the template update mechanism is designed so that the problem of tracking drift caused by interferences from various infrared target changes can be further addressed.

(3) Experiments based on real infrared sequences prove that TSF-SiamMU not only enables advanced tracking results but also runs at 47 FPS on average, achieving the balance between precision and speed.

The following article is divided into four sections. In Section II, the existing target tracking methods are briefly introduced. In section III, the establishment of our tracking model is presented in detail. In section IV, we focus on proving the validity of our method through ablation and comparison experiments. Section V is the summary of the proposed tracker.

## II. RELATED WORK

According to the modeling methods of target appearance, we can divide the existing research of target tracking methods into two categories: generative model-based trackers and discriminative model-based trackers. Typical generative trackers such as Kalman filter [12], particle filter [13] and mean shift [14], apply online feature learning to establish appearance models and then search for the region with minimum reconstruction error in subsequent frames as target position by template matching. However, these types of methods are weaker than discriminative model-based methods in accuracy, as a result of ignorance of background information and insufficient utilization of image information. Discriminative trackers transform tracking problem into a binary classification problem, which leverages feature information in the background by distinguishing between target from background. So far, there have been two mainstreams: correlation filtering methods and deep learning methods. Here, we would like to focus on discussing these two kinds of trackers as follows.

As for the correlation filtering-based approaches, Bolme et al. [15] first introduced the concept of correlation filtering to target tracking field by constructing a new filter which correlates target and subsequent image based on two-dimensional

Gaussian distribution response, thus ensuring a substantial increase in tracking quality and tracking speed. Immediately afterwards, Henriques et al. [16] proposed to map ridge regression in linear space to high-dimensional nonlinear space using kernel functions, as well as a novel cyclic sampling structure, so that the tracking performance can be significantly improved due to high-dimensional nonlinear classification under dense sampling. Following this, various target tracking algorithms based on the traditional framework of correlation filter have emerged. Danelljan et al. [17] adopted a multi-feature fusion mechanism based on KCF to train the scale filter and position filter for target scale estimation and target localization respectively, which can better cope with the scale changes occurring in tracking process. In general, although this kind of correction filter algorithms is fast, it is not easy to maintain the balance between tracking speed and accuracy.

Though researchers had realized the crucial importance of robust and accurate features for the construction of a target appearance model, there was no alternative before to replace such manually designed features that always have flaws. Fortunately, with the development of deep learning, neural networks have significant advantages in feature extraction, which exactly fits the requirements of model design in target tracking tasks. Ma et al. [18] first introduced deep learning into correlation filtering-based trackers and replaced histogram of oriented gradient (HOG) features with hierarchical convolutional features (HCFs) in the trained VGG-19, which finally localized the target by weighted feature maps that fuses both shallow and deep features. Inspired by HCF, Danelljan et al. [19] applied the implicit interpolation to expand feature channels of different resolutions to the higher dimensional continuous spatial domain, and then the object of interest is successfully localized by using Hessian matrix. Despite the advantages of overly complex feature combinations, they may reduce the running speed and increase the risk of overfitting. In order to increase the speed without sacrificing accuracy, Danelljan et al. [20] then proposed a factorization convolution method to simplify the feature extraction dimension and a Gaussian mixture model to merge similar samples; they also designed a model updating strategy against shading challenges based on the framework of C-COT.

Nevertheless, correlation filtering-based trackers still have significant limitations when treating targets with complex appearance, thus a new tracking framework is needed to exploit the full strength of deep learning when extracting features. Tao et al. [21] were the first to propose the Siamese network-based tracker, which learns a matching function by offline training and then locates the target by using the function to calculate the score of template frames and sampled search frames. To make the most of target features, Bertinetto et al. [8] went a step further by using a novel fully-convolutional Siamese network and a tracking approach that employs both offline training and online tuning, which has become the basis for future improvements in Siamese network. In order to improve the generalization performance of the network, He et al. [22] divided the antecedent feature extraction network into two different networks, named semantic branch and appearance branch, which are separately trained to keep the heterogeneity

of the two types of features. To overcome the interference of scale variation, Li et al. [23] brought region proposal network (RPN) into Siamese network based on SiamFC, improving tracking quality by separating localization process into classification and regression branch. Considering that the shallow backbone network in SiamRPN is difficult to extract specific and comprehensive target features, a modern depth network called ResNet was applied by Li et al. [9], in which the translational invariance was overcome, and the problem of asymmetry in two branches was addressed by using uniform sampling and multiple layers.

Although accuracy has been improved by introducing RPN, such anchor-based trackers wasted considerable time in training the model and coped poorly with large scale variations owing to the addition of hyper-parameters of anchor boxes. To deal with the problem, Chen et al. [24] proposed a based-anchor-free Siamese tracker which views tracking problems as a parallel classification and regression problem and thus directly classified objects and regress their bounding boxes. For the purpose of solving the issue of poor robustness of the anchor free method, Zhang et al. [25] proposed a feature alignment-based tracker using different sampling strategies in classification and regression branches. Focusing on how to make the features extracted from the Siamese network more discriminative, Xu et al. [26] applied a new hierarchical convolution fusion network to take advantage of both shallow spatial information and deep semantic information, a channel attention module to selectively enhance the feature channels of the target, and an adaptive update mechanism based on negative template pool to further distinguish the target from the above-mentioned interference of appearance similarity. Since many of the extracted features were useless, Yu et al. [27] introduced various attentional mechanisms to the Siamese tracker, applying not only self-attention module to enrich the contextual information but also mutual attention module to interact the information between template and search region before correlation operation. Enlightened by the occurrence of transformer model [28], Chen et al. [29] proposed a new feature fusion Siamese tracker based on attention mechanism. By repeatedly using the double cross-notice feature enhancement module for feature fusion and finally fusing the features together with the additional cross-feature enhancement module, the tracker addressed the challenge that inter-correlation operations lose semantic information and easily lead to local optimum instead of global optimum. To deal with the problem of unavoidably ignorance in the integrity of objects caused by adopting the pixel-to-pixel attention strategy on flattened image features in existing transformer-based approaches, Song et al. [30] introduced multi-scale cyclic shifting window attention mechanism to transformer architecture, which expands the window samples with positional information and thus greatly improves the accuracy.

### III. METHOD

In this section, we mainly introduce the theory of our TSF-SiamMU tracker. Section III-A is an overview of the proposed tracking framework; the twofold structured features network

is explained in detail in section III-B; on regard of the interferences from appearance changes, a multi-template update module based on template update mechanism is reported in section III-C; the overall procedure of our tracking method is given as a summary in section III-D.

#### A. Overview

The architecture of the proposed TSF-SiamMU network is shown in Fig. 1. The main network consists of two parts: the backbone where the features are extracted and RPN [23] which performs bounding box prediction. The backbone, namely, the twofold structured features network, is a kind of Siamese network architecture composed of a template branch and instance branch. The two inputs branches are a pair of image patches cropped from the first frame and the current frame, i.e., template and instance. It is worth noting that “twofold” implies that the extracted output features in each branch are dual, which are respectively named as shallow features and deep features. While tracking, the optimal template will be changed into the weighted combination of all possible templates by MU module to fit appearance changes. When appearance changes of the target occur during tracking, MU module will output the optimal template of the target by weighting the combination of various templates.

The twofold structured features network is the backbone network of the feature extraction part, where the two branches share the same structure and parameters. Compared with the instance branch, the template branch is equipped with an additional MU module after the backbone outputs two distinguished layers of features, viz., shallow features and deep features.

The RPN consists of a classification branch and a regression branch, the former to handle the target-background classification while the latter to handle the regression values of each anchor position. At the end parts of RPN, there are depth-wise cross correlation layers instead of up-channel cross correlation layers, which convolves the template features with the instance features to achieve sufficient information association and thus to generate a better output correspond map.

Therefore, under the combined influence of the Siamese backbone network and RPN, infrared target tracking can be regarded as a one-shot detection task as follows:

$$\min_W \frac{1}{n} \sum_{i=1}^n L(\zeta(\varphi(x_i; W); F_{MU}(\varphi(z_{in}^{in}; W), \varphi(z_{ac}^{ac}; W), \varphi(z_{cu}^{cu}; W))), l_i) \quad (1)$$

where  $n$  represents the number of data;  $x$ ,  $z_{in}$ ,  $z_{ac}$  and  $z_{cu}$  denotes the instance, the initial template, the accumulated template and the current template, respectively;  $\zeta(\cdot; \cdot)$  and  $\varphi(\cdot; \cdot)$  refer to the function of RPN and Siamese feature extraction network, accordingly;  $l_i$  is the real label of each candidate region estimated by the tracker; and  $F_{MU}(\cdot; \cdot; \cdot)$  is used to update the template by fusing all three template features, which will be discussed in detail in section III-C. More specifically, we argue that the average loss  $L$  is crucial to obtain the parameter  $W$ .

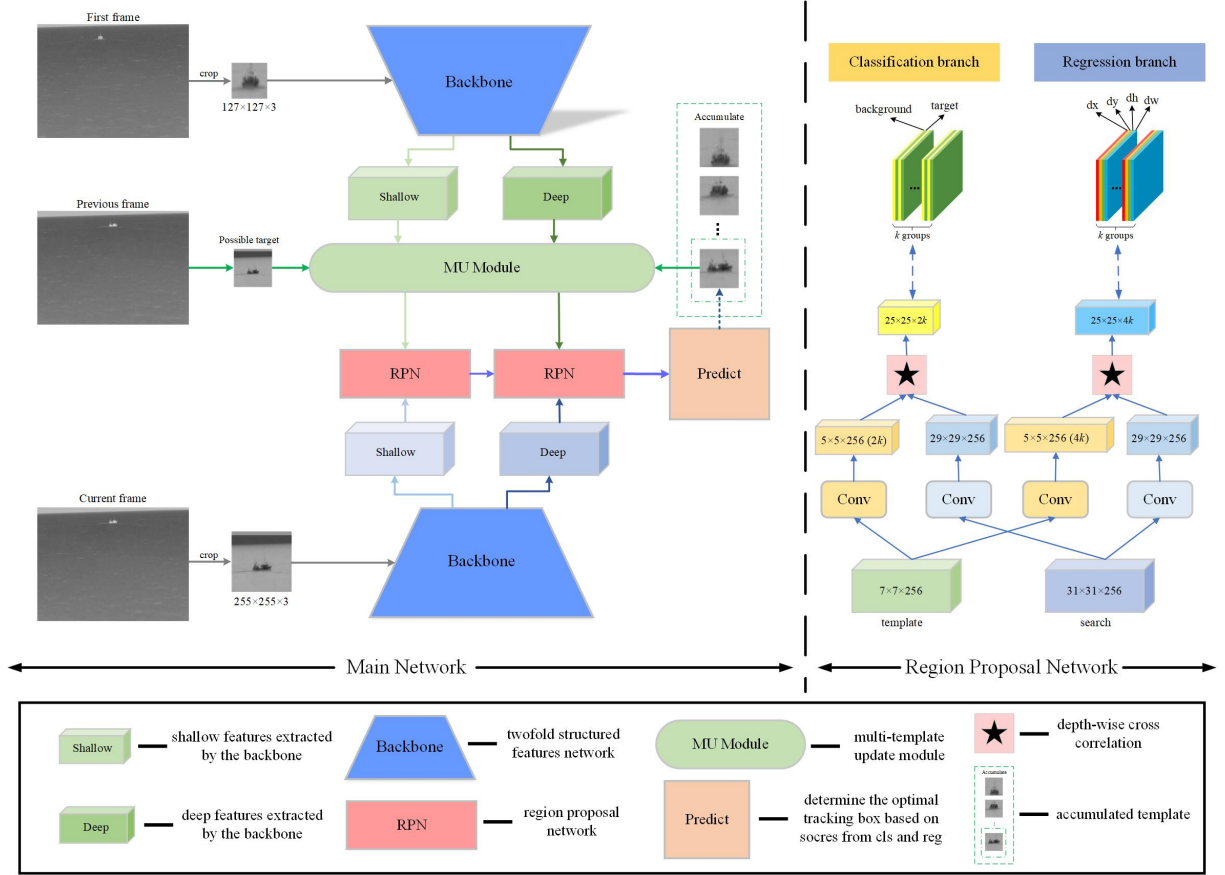


Fig. 1. The framework of the proposed TSF-SiamMU network. The left sub-figure shows its main structure, and the right one shows the structure of each RPN.

### B. Twofold Structured Features Network

Inspired by the success of deep neural networks in Siamese trackers, we adopt ResNet-50 [31] instead of AlexNet [32] as our base feature extraction network. To make the most of the feature representation capability of ResNet-50, we design a novel backbone network called twofold structured features network. As shown in Fig. 2, the presented network is composed of several layers and the subsequent adaptive fusion operation. We note that most previous Siamese trackers usually utilize features of last three layers to present the target, since these layers are at the same spatial resolution and easy to apply. However, as the network goes deeper, the extracted target features tend to convey more semantic information than spatial information, which is prejudicial to infrared target tracking. As a result of lacking details such as color and texture, the semantic information of the infrared target is less discriminative, making spatial information more significant in infrared target tracking [10]. In addition, the extracted features of various layers are always a mixture of shallow spatial information and deep semantic information, yet we expect the features fed into the RPN to be more distinct and focused to better detect the target from the appearance and location separately. The factors mentioned above make it difficult for the tracker to robustly distinguish the target in complex infrared scenes.

In order to obtain more distinctive and robust features

for infrared target tracking, our proposed backbone network additionally employs a relatively shallow layer named Layer1 in ResNet-50 as a supplement to commonly used deeper layers and combines all these layers in a novel manner. Hence, the tracker is able to have access to a wealth of spatial information that facilitates the location of the infrared target. To make it clear, we first explain where our shallow and deep features come from. All layers are made up of several similar convolution combination and downsampling operation, both of which contain different types of convolution operations, normalization and ReLU activation function. Assume that  $CN_{convkernel}^{noutputchannel}$  represents a single combination of convolution operation and batch normalization operation, in which the superscript refers to the output channel of the convolution while the subscript refers to the convolution kernel size, the structure of four layers for feature extraction can be formulated as follows:

$$\begin{cases} layer1 = [CN_{1 \times 1}^{64}; CN_{3 \times 3}^{64}; CN_{1 \times 1}^{256}] \times 3 \\ layer2 = [CN_{1 \times 1}^{128}; CN_{3 \times 3}^{128}; CN_{1 \times 1}^{512}] \times 4 \\ layer3 = [CN_{1 \times 1}^{256}; CN_{3 \times 3}^{256}; CN_{1 \times 1}^{1024}] \times 6 \\ layer4 = [CN_{1 \times 1}^{512}; CN_{3 \times 3}^{512}; CN_{1 \times 1}^{2048}] \times 3 \end{cases} \quad (2)$$

where  $n$  represents the number of sub-layers, and  $[\cdot; \cdot; \cdot]$  denotes the structure of a single sub-layer.  $[\cdot; \cdot; \cdot] \times n$  indicates the superposition of sub-layers.

Furthermore, we define  $F_1 \in R^{31 \times 31 \times 256}$ ,  $F_2 \in R^{15 \times 15 \times 512}$ ,  $F_3 \in R^{15 \times 15 \times 1024}$  and  $F_4 \in R^{15 \times 15 \times 2048}$  as



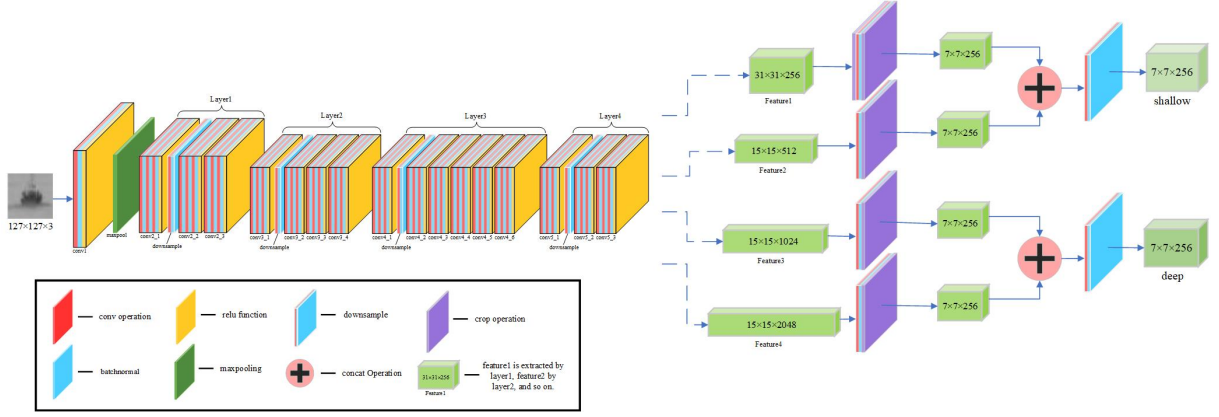


Fig. 2. Structure of the hierarchical convolution fusion network, in which a combination of feature maps from Conv3, Conv4 and Conv5 is utilized to represent the target.

the feature map extracted by Layer1, Layer2, Layer3 and Layer4, separately. As what we design,  $F_1$  and  $F_2$  carry more spatial information while  $F_3$  and  $F_4$  prevail in semantic information. In order to aggregate and then make sufficient use of the varied advantageous information in four feature maps, we need to apply several steps to capture and identify shallow features and deep features. Above all, we convert the four feature maps to the same spatial resolution and feature channels using function  $CR(\cdot)$  and function  $DS(\cdot)$ , where  $CR(\cdot)$  means crop operation to decrease the spatial resolution and  $DS(\cdot)$  denotes downsampling operation to reduce the channel dimension. It is important to note that the initial spatial resolution of  $F_1$  differs from other initial feature maps, as a result of which there is an extra crop operation for  $F_1$  to apply before concatenation operation. After all the feature maps reach the size of  $7 \times 7 \times 256$ , we subsequently use a concatenation operation named  $Concat(\cdot; \cdot)$  to connect the feature maps in series in the direction of channel. At last, another downsampling operation is applied to recover the feature map to the size of  $7 \times 7 \times 256$ , which eases the computational burden and still captures the entire target region. The whole progress mentioned above can be expressed as the following formula:

$$\begin{cases} F_{shallow} = DS(Concat(CR(DS(CR(F_1))), CR(DS(F_2)))) \\ F_{deep} = DS(Concat(CR(DS(F_3)), CR(DS(F_4)))) \end{cases} \quad (3)$$

where  $F_{shallow}$  represents the shallow feature map extracted by the backbone while  $F_{deep}$  denotes the deep one. Either of them not only provides a decent representation of the target but is also the ideal size for both online tracking and offline training.

### C. Multi-template Update Module

Due to large and frequent appearance changes, failing to update the template is a serious concern for traditional Siamese trackers. However, most linear update methods, where the template is updated as a running average with exponentially decaying weights over time, are too simple to allow for a flexible update mechanism when the infrared target undergoes

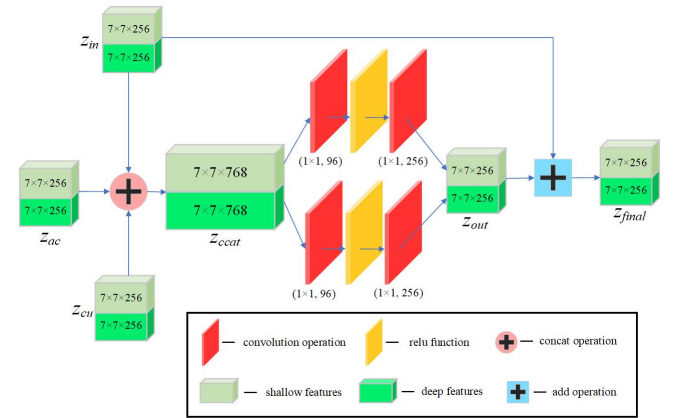


Fig. 3. Structure of the multi-template update module, in which initial template, accumulated template and current template are applied as supplements to the optimal template for target tracking.

complex appearance changes. Thus, we focus on designing a multi-template update module to obtain the optimal template suitable for tracking.

In contrast to linear update methods, we adopt a simplified residual network to combine the templates in a far more reasonable manner throughout the tracking progress. In the first step, the three different feature maps, all consisting of shallow and deep features, are connected in series in the direction of channel. Once the concatenation operation is done, several convolution layers are applied to extract the detailed information in the accumulated template and the current template. It is necessary to point out that shallow features and deep features are handled in separate sub-networks with the same structure but varying parameters. Considering that the initial template provides the most reliable information, the final template is a combination of the initial template and the output template extracted by the convolutional network. The final template is not only the optimal template to measure the bounding box for tracking in the current frame, but is also the accumulated template to calculate the optimal template in the

next frame. The updating progress is formulated as follows:

$$\begin{cases} z_{final} = MU(Concat(z_{in}, z_{ac}, z_{cu})) + z_{in} \\ MU = CV(RE(CV(\cdot))) \end{cases} \quad (4)$$

where  $z_{in}$ ,  $z_{ac}$  and  $z_{cu}$  denote the initial ground-truth template, the last accumulated template and the current template extracted from the predicted target location, respectively.  $CV(\cdot)$  represents the convolution operation while  $RE(\cdot)$  represents the ReLU activation function.  $Concat(\cdot; \cdot; \cdot)$  refers to the concatenation operation. The final template  $z_{final}$  is likewise composed of shallow features and deep features.

The multi-template update module is trained to predict the target template  $z_{i+1}^{GT}$  which should be the best matching template to use when searching for the target in the next frame. Hence, to begin with, we extract the ground truth frame through the backbone (see Fig. 2) to obtain  $z_{i+1}^{GT}$ . What is more, minimizing the Euclidean distance between the updated template and the ground-truth template is the key to derive  $W$ , just as what is defined below:

$$\min_W \|F_{MU}(z_0^{in}, z_i^{ac}, z_i^{cu}, W) - z_{i+1}^{GT}\|_2 \quad (5)$$

where  $F_{MU}(\cdot; \cdot; \cdot; W)$  is used to update the template by fusing the three template features.  $\|\cdot\|$  denotes the  $L_2$  norm or Euclidean distance.

#### D. General tracking process

Once we obtain the search instance and the optimal template, the classification maps and the regression maps are naturally available via RPN (see Fig. 1). Since the shallow layers can capture fine-grained information useful for precise localization while the deep layers can encode abstract semantic information conducive to target recognition, we apply multiple adaptive prediction in order to take full advantage of multi-level features. We set the weights  $\alpha$  and  $\beta$  which correspond to each map and are capable to be optimized together with the backbone network. The formula can be expressed as follows:

$$\begin{cases} P_{cls}^{all} = \alpha_s P_{cls}^{shallow} + \alpha_d P_{cls}^{deep} \\ P_{reg}^{all} = \beta_s P_{reg}^{shallow} + \beta_d P_{reg}^{deep} \end{cases} \quad (6)$$

where  $P_{cls}$  and  $P_{reg}$  represent the classification maps and the regression maps, respectively. The classification branch scores each location calculated by the regression branch and the top scorer is the most likely to be the target location.

To give a clear description of our proposed tracker, the main steps are summarized in Algorithm 1 in table I.

### IV. EXPERIMENTAL RESULTS

In this section, we demonstrate the validity and sophistication of our proposed tracker through diverse experiments. First of all, the datasets we used to evaluate trackers are briefly introduced in section IV-A. Then, we give some implementation details of offline and online acts in section IV-B. Section IV-C is an introduction of the evaluation criteria to quantify trackers' performance. We carry out an ablation experiment in section IV-D in order to prove the effectiveness of each component of our tracker. In section IV-E, other state-of-the-art trackers are compared with our tracker.

#### A. Datasets

In our experiments, the VOT-TIR 2016 [33] dataset is used to test the performance of our method. Compared to VOT-TIR 2015 [34], VOT-TIR 2016 removes or modifies several sequences that are too easy for tracking and adds quite a number of challenging sequences, in which blur or motion change is a significant problem. In addition to the bounding box annotations, part of the local attributes and global attributes, i.e., size change, motion change, dynamic change, blur, scale variation, scene complexity and so on, are introduced in VOT-TIR 2016 to present a better assessment of the comprehensive performance of the tracker. Fig. 4 shows the first frames of part of the sequences in VOT-TIR 2016, where the red rectangle marks the target to be tracked.

#### B. Implementation Details

We train our proposed backbone network with five large-scale datasets, including COCO [35], GOT10k [36], LaSOT [37], ImageNet VID and ImageNet DET [38] in order to learn how to measure the similarities between objects for tracking. In both offline training and online tracking, we crop the frame in a fixed mode where the size of a template patch is  $127 \times 127$  pixels and the size of an instance patch is  $255 \times 255$  pixels. What is more, a stride-reduced ResNet-50 is applied as the pretrained network to initialize the parameters of the backbone network which is further trained with stochastic gradient descent (SGD). The training is performed over 50 epoches where a warmup learning rate of 0.001 is used in the first 5 epoches and the learning rate exponentially decays from 0.005 to 0.0005 for the last 15 epoches. Noticing that the multi-template update module contains a neural network which is different from the common backbone network, we apply a unique training strategy in next stage. Since the proposed multi-template update module has fewer parameters than the backbone network, we train this module with one single dataset named LaSOT to measure the optimal template for tracking. We train the module for 50 epochs with SGD and the learning rate is decreased logarithmically at each epoch from  $10^{-7}$  to  $10^{-8}$ .

Our experiments are implemented using PyTorch on a PC with NVIDIA GeForce RTX 3080Ti GPU, Intel i7-11700 CPU and 16GB RAM. The average testing speed of the proposed tracker can reach 47 FPS.

#### C. Evaluation Criteria

To evaluate the performance of the proposed method precisely, we adopt success rate and precision to measure the tracking effectiveness. Above all, for each frame in a sequence, we define overlap score (OS) to represent the intersection rate of the predicted region and the ground-truth region, as well as center pixel error (PE) [39] [40] to represent the Euclidean distance in pixels between the predicted target center position and the ground-truth center position. The formulae of these two metrics are as follows:

$$OS = \frac{|B_t \cap G_t|}{|B_t \cup G_t|} \quad (7)$$

TABLE I  
ALGORITHMS FOR THE PROPOSED TSF-SIAMMU TRACKER.

---

**Algorithm 1** Main steps of the proposed TSF-SiamMU tracker

---

**Input:** The first frame with the target  $z_0$ , initial bounding box  $(x_0, y_0, w_0, h_0)$ , and the current frame  $x_i$ .

**Output:** The predicted bounding box  $(x_i, y_i, w_i, h_i)$ .

**Repeat**

1. Crop the first frame  $z_0$  based on the initial bounding box  $(x_0, y_0, w_0, h_0)$ , extract it by Eq. 3, and we get  $z_{in}$ .
2. Crop the current frame  $x_i$ , extract it by Eq. 3 the same as what we do to the template branch, and we get  $x_{cu}$ .
3. Estimate the optimal template  $z_{final}$  via Eq. 4, namely the Multi-template Update Module.
4. Calculate the  $P_{cls}^{all}$  and  $P_{reg}^{all}$  via Eq. 6.
5. Calculate the highest scorer and its corresponding position via  $P_{cls}^{all}$  and  $P_{reg}^{all}$ , and predict the bounding box  $(x_i, y_i, w_i, h_i)$ .

**Until** End of the video sequence.

---

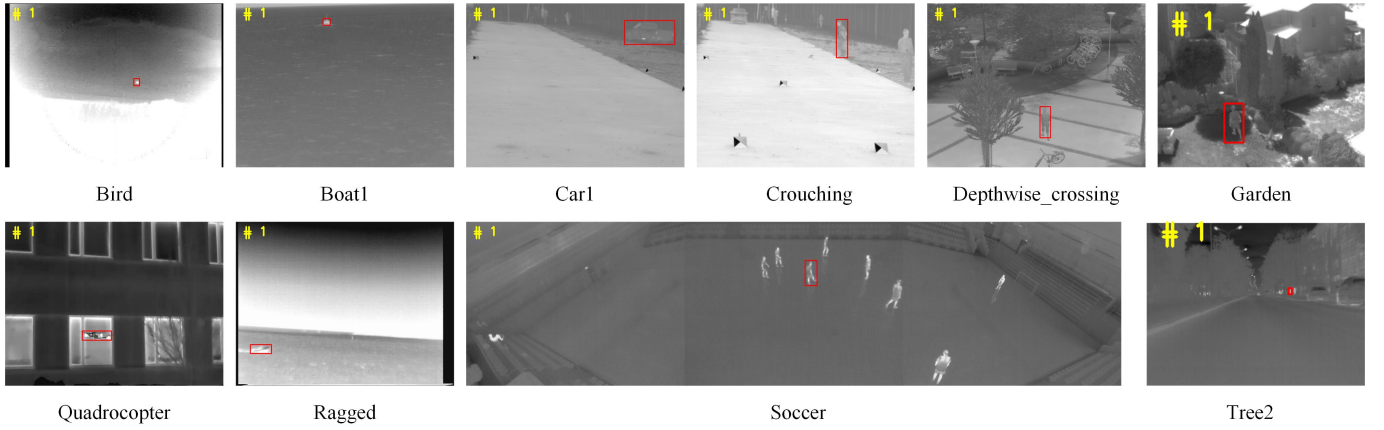


Fig. 4. First frame of part of the sequences in VOT-TIR 2016. The target is marked by a red rectangle.

$$PE = \sqrt{(x_t^B - x_t^G)^2 + (y_t^B - y_t^G)^2} \quad (8)$$

where  $B_t$  and  $G_t$  denote the predicted bounding box and the area of ground truth, respectively. The coordinates of the centers of  $B_t$  and  $G_t$  are denoted as  $(x_t^B, y_t^B)$  and  $(x_t^G, y_t^G)$ , correspondingly.

Then, with the thresholds  $OS_{th}$  and  $PE_{th}$  configured, the success rate  $S_i$  and the precision rate  $P_i$  in a given sequence can be calculated as the ratio of frames  $k_i$  above or below the threshold to the total number of frames  $n_i$ . The definitions are outlined below:

$$S_i = \frac{k_{OS > OS_{th}}}{n_i} \quad (9)$$

$$P_i = \frac{k_{PE < PE_{th}}}{n_i} \quad (10)$$

where  $k_{OS > OS_{th}}$  denotes the number of frames whose  $OS$  values are larger than the set threshold  $OS_{th}$ , and  $k_{PE < PE_{th}}$  denotes the number of frames whose  $PE$  values are smaller than the set threshold  $PE_{th}$ . By calculating the success rates under different  $OS_{th}$  thresholds, a success plot is obtained, in which the area under curve is reported to synthesize all these different success rates. Also, the precision plot can be drawn in a similar way, and we usually report the representative precision at threshold  $PE_{th}$  of 20 pixels.

#### D. Ablation Analysis

In this section, the effectiveness of each optimization component in our approach is verified through ablation analysis. We carry out an internal comparison experiment on VOT-TIR 2016 dataset to evaluate the three variants of our tracker.

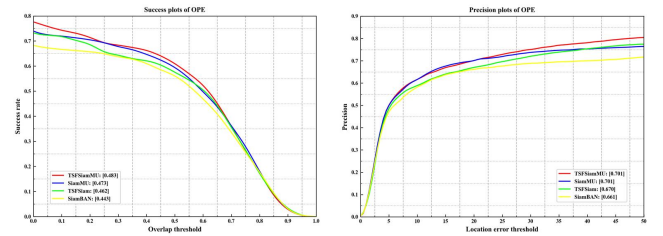


Fig. 5. Success plots and precision plots of the ablation experiments conducted on VOT-TIR 2016.

Since all modified components are added on the basis of the baseline tracker called SiamBAN, we compare our variants with SiamBAN and our proposed tracker called TSF-SiamMU to prove that each of our improvements is generally positive. First, a tracker named TSF-Siam, which only adds twofold structured features network, is compared with SiamBAN to check that twofold structured features network is effective. Subsequently, in a bid to prove the multi-template update module works, SiamMU which is only equipped with the

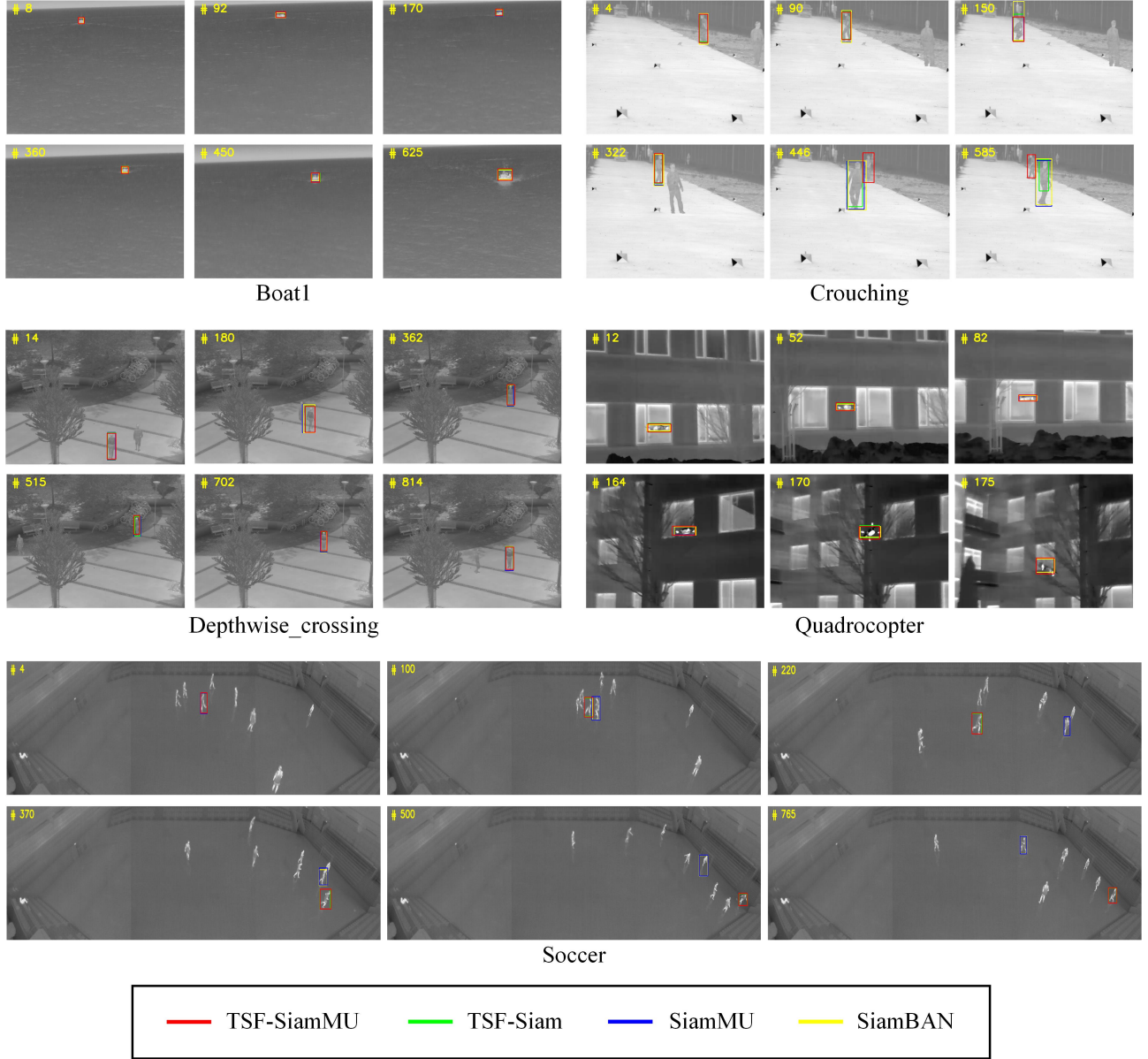


Fig. 6. Part of the visualization results of the ablation experiments conducted on VOT-TIR 2016.

TABLE II  
ABLATION ANALYSIS OF OUR METHOD ON VOT-TIR 2016,  
WHERE TSF AND MU DENOTE TWOFOLD STRUCTURED  
FEATURES NETWORK AND MULTI-TEMPLATE UPDATE  
MODULE, RESPECTIVELY.

Component	SiamBAN	TSF-Siam	SiamMU	TSF-SiamMU
TSF		✓		✓
MU			✓	✓
AUC	0.443	0.462	0.473	0.483
Precision	0.661	0.670	0.701	0.701

multi-template update module is compared with SiamBAN. Finally, a comprehensive comparison of TSF-Siam, SiamMU and TSF-SiamMU is performed in order to demonstrate that all of our optimization components are uncontradictory and synergistic once they are combined all together, where TSF-

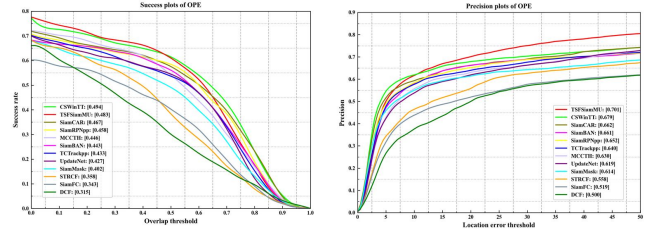


Fig. 7. Success plots and precision plots of the external comparison experiments conducted on VOT-TIR 2016.

SiamMU is our proposed tracker.

Listed in Table II are results of ablation experiments on VOT-TIR 2016. In addition, Fig. 5 shows the success plots and precision plots of one-path evaluation (OPE) [41] on VOT-TIR 2016. From the table and the graph, it is apparent that



TABLE III  
COMPARISON BETWEEN TSF-SIAM AND STATE-OF-THE-ART TRACKERS ON VOT-TIR 2016. DATA MARKED IN RED, GREEN AND BLUE DENOTES THE FIRST, SECOND, AND THIRD, RESPECTIVELY.

Tracker	TSF-SiamMU	SiamCAR	TCTrackerpp	CSWinTT	SiamRPNpp	UpdateNet	SiamBAN	SiamMask	SiamFC	MCCTH	STRCF	DCF
AUC	<b>0.483</b>	<b>0.467</b>	0.434	<b>0.494</b>	0.458	0.427	0.443	0.402	0.343	0.446	0.359	0.315
Precision	<b>0.701</b>	<b>0.662</b>	0.640	<b>0.680</b>	0.652	0.619	0.661	0.614	0.519	0.631	0.558	0.500
FPS	47.4	71.1	<b>99.1</b>	9.5	76.8	<b>118.5</b>	80.0	65.8	71.9	21.4	24.1	<b>509.7</b>

each optimization component of our method has a considerable contribution to the improvement of tracking performance. To begin with, it is plain to witness that TSF-Siam outperforms SiamBAN in terms of AUC and precision. Especially, both the AUC and precision increase by nearly 4.3% and 1.4% compared with the baseline algorithm, which demonstrates that twofold structured features network facilitates the extraction of robust features for the infrared target. Next, when adopting the multi-template update module to the baseline algorithm, the AUC and precision of SiamMU are enhanced by 6.8% and 6.1% over SiamBAN, which proves that the multi-template update module is effective for tracking task. Last but not least, although the precision is almost equal for TSF-SiamMU and SiamMU, when it comes to the AUC, TSF-SiamMU gains 4.5% and 2.1% increase compared with TSF-Siam and SiamMU, respectively, which implies that the two components cooperate well with each other.

As shown in Fig. 6, in order to demonstrate the performance of our three variants (TSF-Siam, SiamMU and TSF-SiamMU) and the baseline tracker (SiamBAN) in a more intuitive manner, we visualize their tracking results on several challenging sequences. It is evident that the presented TSF-SiamMU is able to handle complex target variations and locate the target consistently. In some sequences (see “Crouching” and “Soccer”), once the target changes in size, TSF-Siam is prone to tracking drift when it encounters interferences caused by similar deep semantic information in the following tracking. Meanwhile, without the ability of meticulous discrimination between shallow and deep information and thus lack of robust template features, SiamMU is vulnerable to those confusing similar targets in close proximity to each other, which brings instability to the results of infrared tracking. Finally, equipped with twofold structured features network and multi-template update module, TSF-SiamMU not only runs in a more stable way (see sequence “Boat1”, “Depthwise\_crossing” and “Quadrocopter”) but also more robust to those complex tracking scenes (see sequence “Crouching” and “Soccer”).

#### E. External Comparison

In this section, we compare our proposed tracker with another 11 tracking algorithms to demonstrate that our method achieves the better performance on VOT-TIR 2016 against the state-of-the-art algorithms. The 11 tracking algorithms can be divided into three categories: CF trackers including DCF [16], STRCF [42] and MCCTH [43]; Siamese trackers consisting of SiamFC [8], SiamMask [44], UpdateNet [11], SiamRPNpp [9], SiamCAR [45], SiamBAN [24] and TCTrackerpp [7]; and one transformer tracker CSWinTT [30].

The success plots and precision plots of OPE on VOT-TIR 2016 are shown in Fig. 7. More detailed results are listed in Table III. Note that all parameter values of trackers for comparison are default parameters set by their authors. Among these methods, our TSF-SiamMU tracker achieves the second AUC of 0.483, which is only 2.2% lower than that of the non-real-time tracker CSWinTT and 3.4% higher than that of the real-time tracker SiamCAR. Since CSWinTT runs at 9.5 FPS far behind the real-time requirement of 30 FPS, it is acceptable that our method almost catches up with CSWinTT which obtains the AUC of 0.494. CF trackers fall far behind our method obviously, where the best CF tracker MCCTH attains the AUC of 0.446. SiamCAR and SiamRPNpp achieve 0.467 and 0.458 in terms of AUC, respectively, which are top two Siamese trackers for comparison but still not as strong as our method. In addition, it is worth noting that our tracker acquires the Precision of 0.701, which comes first among all mentioned trackers even including CSWinTT. For remaining Siamese trackers, SiamCAR stands out with its superior precision of 0.662, however still having 5.9% decrease when compared with our method. Although the CF tracker MCCTH reaches the precision of 0.631, it is also 11.1% lower than ours, which further implies the advance of our method in accuracy. Moreover, the results of tracking speed are listed in the third rows of Table III. Our proposed TSF-SiamMU tracker achieves a speed of 47.4 FPS, satisfying the requirement of real-time tracking. Whereas, these trackers for comparison either perform the equivalent performance to TSF-SiamMU but hardly meet real-time requirements, as in the case of CSWinTT; or they meet real-time requirements yet are nowhere near as well as ours in terms of tracking performance, as in the case of SiamCAR and SiamRPNpp. In conclusion, we believe that our tracker strikes a balance between tracking performance and tracking speed, emerging as a new outstanding tracker for infrared target tracking.

To analyze the influence of different tracking challenges to our trackers in VOT-TIR 2016, several groups of comparison experiments are carried out on sequences with challenges of motion change, size change, blur and scale variation. All evaluation sequences in these four groups for experiments are selected from VOT-TIR 2016 according to the given attributes. The comparison results are given in Fig. 8. First, our tracker is the best tracker in terms of both AUC and precision when encountering objects with motion changes, thanks to the design of our feature extraction network which separates shallow and deep features. In contrast, even though CSWinTT has strong feature extraction capability at the expense of tracking speed, it makes mistakes from time to time due to its lack of fine distinction between spatial

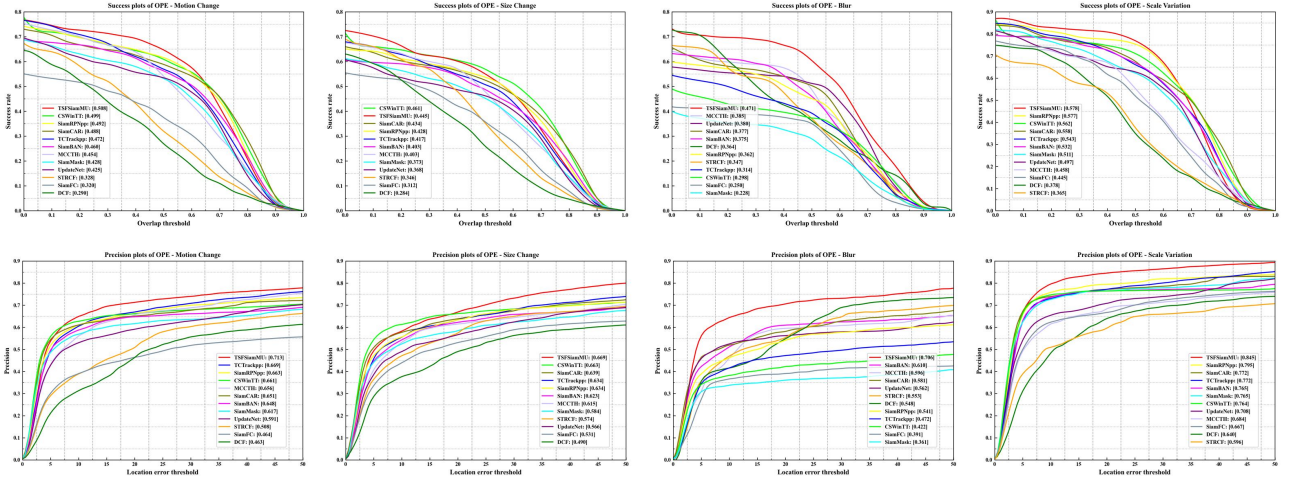


Fig. 8. Success plots and precision plots of the external comparison experiments conducted on sequences with different challenges.

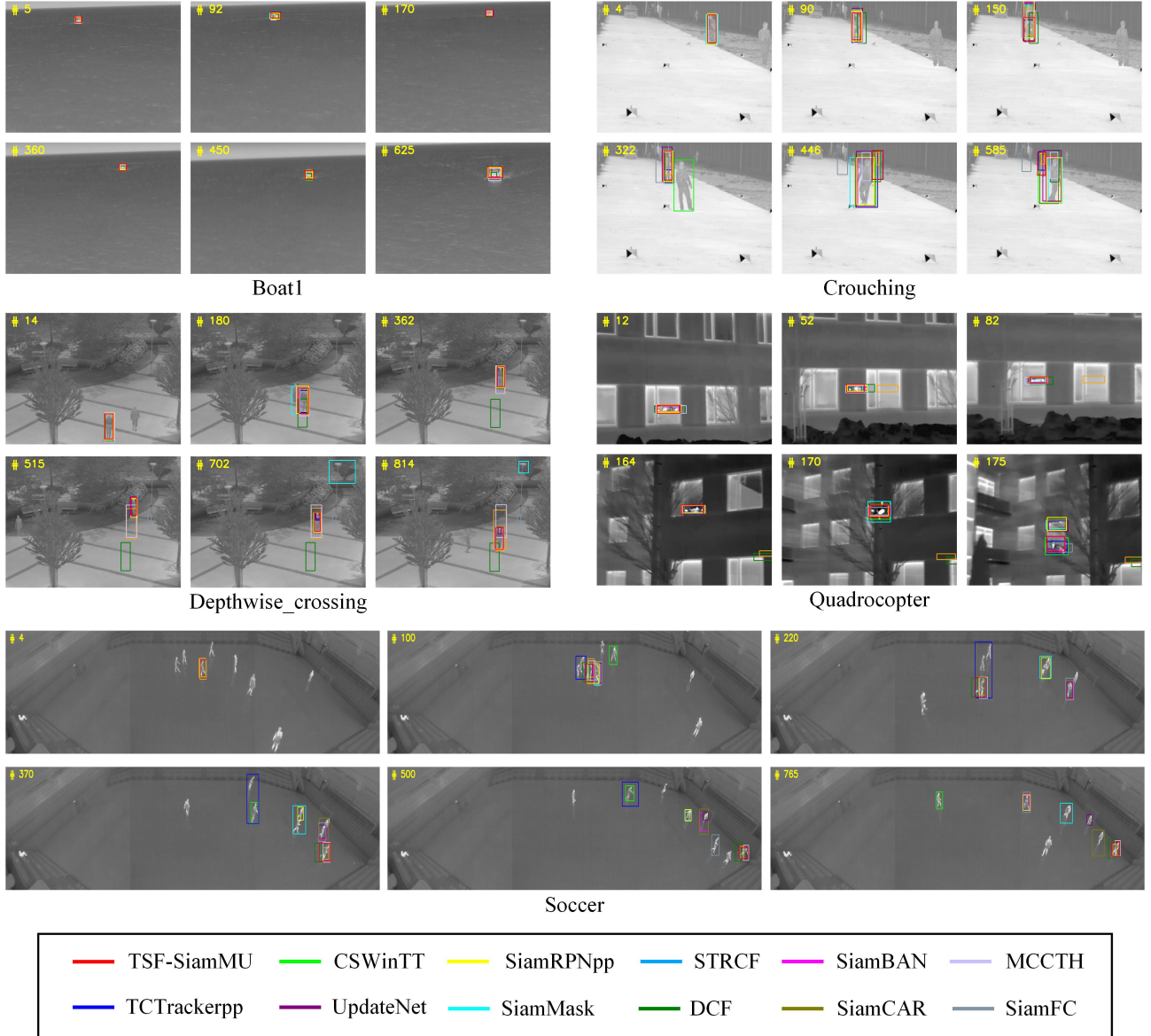


Fig. 9. Part of the visualization results of the external comparison experiments conducted on VOT-TIR 2016.

and semantic information of the target, thus resulting in the inferior performance to TSF-SiamMU in sequences of motion changes. Second, owing to the inclusiveness to size changes in targets by using multi-template update module, our method takes the second place on AUC and first place on precision. Relatively, trackers which utilize nothing or simple linear template update strategy, such as SiamCAR and SiamBAN, is sensitive to the appearance changes of target, especially complex shape changes. Third, it is plain to see that our TSF-SiamMU tracker gets the highest AUC and precision when it comes to those blur sequences. Despite the difficulty of these sequences and the fact that none of the trackers get the satisfied performance, our method makes a step forward nevertheless thanks to its comprehensive ability of deriving the semantic information from the background. Besides, we can see clearly that either the AUC or the precision of TSF-SiamMU ranks first in sequences with frequent scale variation. Overall, TSF-SiamMU does have the outstanding performance, which can be found from the selected visualization results shown in Fig. 9. When the target comes across motion changes, many trackers, including Siamese trackers, suffer the risk of tracking drift. In particular, it is worsened if the infrared target encounters occlusion, blur or size changes during movement. This conclusion can be observed from the tracking results in sequences “Crouching”, “Depthwise\_crossing” and “Soccer”. In terms of sequences with scale variation challenges, such as “Boat1” and “Quadrocopter”, the changes in target appearance information are coherent and continuous, so the tracking accuracy must be maintained at a high level throughout the tracking process. In this regard, TSF-SiamMU not only deploys twofold structured features network to make full use of the shallow and deep features of the target, but also applies multi-template update module to attenuate the interference of target appearance changes. All in all, both quantitative and visualization results indicate that our TSF-SiamMU tracker is capable of standing up to other state-of-the-art methods in complex infrared scenes.

In Fig. 9, we give the visualization results on 7 representative sequences, including the challenges of deformation, occlusion, and appearance similarity, to compare our tracker against to some state-of-the-art trackers more intuitively. As we can see, many trackers, especially the Siamese trackers, are easy to fail when coming across objects with similar appearance to the target. In particular, when the target is occluded, the possibility of tracking drift increases rapidly, which can be observed from the tracking results in sequences “Irw01”, “Saturated”, “Crouching”, and “Street”. For sequences “Birds”, “Running\_rhino” and “Score”, in which the target is surrounded by its appearance similar objects throughout the whole tracking process, the continuous changes in the apparent information of the target are the culprit for tracking failure to some extent. To this end, HCFA-Siam not only applies shallow spatial information to enrich the feature of target, but also makes full use of the negative template pool to weaken the role of the appearance similarity interference, thereby balancing the impacts brought from the above-mentioned changes well.

Overall, the visual evaluation indicates that our HCFA-Siam tracker has the ability to perform favorably against to other state-of-the-art methods in complex scenes.

## V. CONCLUSION

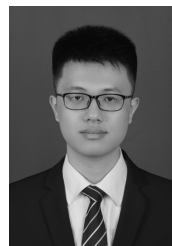
In this article, a twofold structured features-based Siamese multi-update tracker, called TSF-SiamMU, is presented. First of all, we design a novel feature fusion network to extract and make full use of both shallow spatial information and deep semantic information in a comprehensive manner, thereby providing richer and more robust feature representations for infrared target tracking. Further, a multi-template update module is proposed to effectively address the problem of tracking drift caused by the interferences derived from infrared target appearance changes. Finally, both qualitative and quantitative experimental results on VOT-TIR 2016 demonstrate that our method achieves the balance of tracking accuracy and real-time tracking speed against other out-of-the-art trackers. In the future work, we plan to give the Siamese tracker a broader sight in the search branch in order to deal with the more challenging tracking problems, for example, the wide range of target position changes in adjacent frames due to camera motion.

## REFERENCES

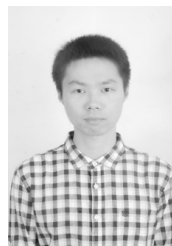
- [1] Q. Liu, D. Yuan, N. Fan, P. Gao, X. Li, and Z. He, “Learning dual-level deep representation for thermal infrared tracking,” *IEEE Transactions on Multimedia*, vol. 25, pp. 1269–1281, 2022.
- [2] S. Du and S. Wang, “An overview of correlation-filter-based object tracking,” *IEEE Transactions on Computational Social Systems*, vol. 9, no. 1, pp. 18–31, 2021.
- [3] M. Wan, X. Ye, X. Zhang, Y. Xu, G. Gu, and Q. Chen, “Infrared small target tracking via gaussian curvature-based compressive convolution feature extraction,” *IEEE Geoscience and Remote Sensing Letters*, vol. 19, pp. 1–5, 2021.
- [4] W. F. Abaya, J. Basa, M. Sy, A. C. Abad, and E. P. Dadios, “Low cost smart security camera with night vision capability using raspberry pi and opencv,” in *2014 International conference on humanoid, nanotechnology, information technology, communication and control, environment and management (HNICEM)*. IEEE, 2014, pp. 1–6.
- [5] M. S. Kristoffersen, J. V. Dueholm, R. Gade, and T. B. Moeslund, “Pedestrian counting with occlusion handling using stereo thermal cameras,” *Sensors*, vol. 16, no. 1, p. 62, 2016.
- [6] A. Gaur, A. Singh, A. Kumar, A. Kumar, and K. Kapoor, “Video flame and smoke based fire detection algorithms: A literature review,” *Fire technology*, vol. 56, pp. 1943–1980, 2020.
- [7] Z. Cao, Z. Huang, L. Pan, S. Zhang, Z. Liu, and C. Fu, “Tctrack: Temporal contexts for aerial tracking,” in *Proceedings of the IEEE/CVF Conference on Computer Vision and Pattern Recognition*, 2022, pp. 14 798–14 808.
- [8] L. Bertinetto, J. Valmadre, J. F. Henriques, A. Vedaldi, and P. H. Torr, “Fully-convolutional siamese networks for object tracking,” in *Computer Vision—ECCV 2016 Workshops: Amsterdam, The Netherlands, October 8–10 and 15–16, 2016, Proceedings, Part II 14*. Springer, 2016, pp. 850–865.
- [9] B. Li, W. Wu, Q. Wang, F. Zhang, J. Xing, and J. Yan, “Siamrpn++: Evolution of siamese visual tracking with very deep networks,” in *Proceedings of the IEEE/CVF conference on computer vision and pattern recognition*, 2019, pp. 4282–4291.
- [10] A. He, C. Luo, X. Tian, and W. Zeng, “A twofold siamese network for real-time object tracking,” in *Proceedings of the IEEE conference on computer vision and pattern recognition*, 2018, pp. 4834–4843.
- [11] L. Zhang, A. Gonzalez-Garcia, J. V. D. Weijer, M. Danelljan, and F. S. Khan, “Learning the model update for siamese trackers,” in *Proceedings of the IEEE/CVF international conference on computer vision*, 2019, pp. 4010–4019.



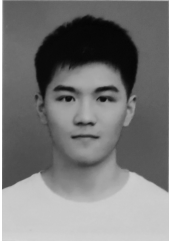
- [12] Z. Zhang and J. Zhang, "A new real-time eye tracking based on nonlinear unscented kalman filter for monitoring driver fatigue," *Journal of Control Theory and Applications*, vol. 8, pp. 181–188, 2010.
- [13] C. Chang and R. Ansari, "Kernel particle filter for visual tracking," *IEEE signal processing letters*, vol. 12, no. 3, pp. 242–245, 2005.
- [14] D. Comaniciu and P. Meer, "Mean shift: A robust approach toward feature space analysis," *IEEE Transactions on pattern analysis and machine intelligence*, vol. 24, no. 5, pp. 603–619, 2002.
- [15] D. S. Bolme, J. R. Beveridge, B. A. Draper, and Y. M. Lui, "Visual object tracking using adaptive correlation filters," in *2010 IEEE computer society conference on computer vision and pattern recognition*. IEEE, 2010, pp. 2544–2550.
- [16] J. F. Henriques, R. Caseiro, P. Martins, and J. Batista, "High-speed tracking with kernelized correlation filters," *IEEE transactions on pattern analysis and machine intelligence*, vol. 37, no. 3, pp. 583–596, 2014.
- [17] M. Danelljan, G. Häger, F. Khan, and M. Felsberg, "Accurate scale estimation for robust visual tracking," in *British machine vision conference, Nottingham, September 1-5, 2014*. Bmva Press, 2014.
- [18] C. Ma, J.-B. Huang, X. Yang, and M.-H. Yang, "Hierarchical convolutional features for visual tracking," in *Proceedings of the IEEE international conference on computer vision*, 2015, pp. 3074–3082.
- [19] M. Danelljan, A. Robinson, F. Shahbaz Khan, and M. Felsberg, "Beyond correlation filters: Learning continuous convolution operators for visual tracking," in *Computer Vision–ECCV 2016: 14th European Conference, Amsterdam, The Netherlands, October 11–14, 2016, Proceedings, Part V 14*. Springer, 2016, pp. 472–488.
- [20] M. Danelljan, G. Bhat, F. Shahbaz Khan, and M. Felsberg, "Eco: Efficient convolution operators for tracking," in *Proceedings of the IEEE conference on computer vision and pattern recognition*, 2017, pp. 6638–6646.
- [21] R. Tao, E. Gavves, and A. W. Smeulders, "Siamese instance search for tracking," in *Proceedings of the IEEE conference on computer vision and pattern recognition*, 2016, pp. 1420–1429.
- [22] A. He, C. Luo, X. Tian, and W. Zeng, "A twofold siamese network for real-time object tracking," in *Proceedings of the IEEE conference on computer vision and pattern recognition*, 2018, pp. 4834–4843.
- [23] B. Li, J. Yan, W. Wu, Z. Zhu, and X. Hu, "High performance visual tracking with siamese region proposal network," in *Proceedings of the IEEE conference on computer vision and pattern recognition*, 2018, pp. 8971–8980.
- [24] Z. Chen, B. Zhong, G. Li, S. Zhang, and R. Ji, "Siamese box adaptive network for visual tracking," in *Proceedings of the IEEE/CVF conference on computer vision and pattern recognition*, 2020, pp. 6668–6677.
- [25] Z. Zhang, H. Peng, J. Fu, B. Li, and W. Hu, "Ocean: Object-aware anchor-free tracking," in *Computer Vision–ECCV 2020: 16th European Conference, Glasgow, UK, August 23–28, 2020, Proceedings, Part XXI 16*. Springer, 2020, pp. 771–787.
- [26] Y. Xu, M. Wan, Q. Chen, W. Qian, K. Ren, and G. Gu, "Hierarchical convolution fusion-based adaptive siamese network for infrared target tracking," *IEEE Transactions on Instrumentation and Measurement*, vol. 70, pp. 1–12, 2021.
- [27] Y. Yu, Y. Xiong, W. Huang, and M. R. Scott, "Deformable siamese attention networks for visual object tracking," in *Proceedings of the IEEE/CVF conference on computer vision and pattern recognition*, 2020, pp. 6728–6737.
- [28] A. Vaswani, N. Shazeer, N. Parmar, J. Uszkoreit, L. Jones, A. N. Gomez, Ł. Kaiser, and I. Polosukhin, "Attention is all you need," *Advances in neural information processing systems*, vol. 30, 2017.
- [29] X. Chen, B. Yan, J. Zhu, D. Wang, X. Yang, and H. Lu, "Transformer tracking," in *Proceedings of the IEEE/CVF conference on computer vision and pattern recognition*, 2021, pp. 8126–8135.
- [30] Z. Song, J. Yu, Y.-P. P. Chen, and W. Yang, "Transformer tracking with cyclic shifting window attention," in *Proceedings of the IEEE/CVF conference on computer vision and pattern recognition*, 2022, pp. 8791–8800.
- [31] K. He, X. Zhang, S. Ren, and J. Sun, "Deep residual learning for image recognition," in *Proceedings of the IEEE conference on computer vision and pattern recognition*, 2016, pp. 770–778.
- [32] A. Krizhevsky, I. Sutskever, and G. E. Hinton, "Imagenet classification with deep convolutional neural networks," *Advances in neural information processing systems*, vol. 25, 2012.
- [33] K. Lebeda, S. Hadfield, R. Bowden *et al.*, "The thermal infrared visual object tracking vot-tir2016 challenge result," in *Proceedings, European Conference on Computer Vision (ECCV) workshops*, 2016.
- [34] M. Felsberg, A. Berg, G. Hager, J. Ahlberg, M. Kristan, J. Matas, A. Leonardis, L. Cehovin, G. Fernandez, T. Vojir *et al.*, "The thermal infrared visual object tracking vot-tir2015 challenge results," in *Proceedings of the IEEE international conference on computer vision workshops*, 2015, pp. 76–88.
- [35] T.-Y. Lin, M. Maire, S. Belongie, J. Hays, P. Perona, D. Ramanan, P. Dollár, and C. L. Zitnick, "Microsoft coco: Common objects in context," in *Computer Vision–ECCV 2014: 13th European Conference, Zurich, Switzerland, September 6–12, 2014, Proceedings, Part V 13*. Springer, 2014, pp. 740–755.
- [36] L. Huang, X. Zhao, and K. Huang, "Got-10k: A large high-diversity benchmark for generic object tracking in the wild," *IEEE transactions on pattern analysis and machine intelligence*, vol. 43, no. 5, pp. 1562–1577, 2019.
- [37] H. Fan, L. Lin, F. Yang, P. Chu, G. Deng, S. Yu, H. Bai, Y. Xu, C. Liao, and H. Ling, "Lasot: A high-quality benchmark for large-scale single object tracking," in *Proceedings of the IEEE/CVF conference on computer vision and pattern recognition*, 2019, pp. 5374–5383.
- [38] O. Russakovsky, J. Deng, H. Su, J. Krause, S. Satheesh, S. Ma, Z. Huang, A. Karpathy, A. Khosla, M. Bernstein *et al.*, "Imagenet large scale visual recognition challenge," *International journal of computer vision*, vol. 115, pp. 211–252, 2015.
- [39] Y. Wang, S. Hu, and S. Wu, "Visual tracking based on group sparsity learning," *Machine Vision and Applications*, vol. 26, pp. 127–139, 2015.
- [40] Y. Lu, T. Wu, and S. Chun Zhu, "Online object tracking, learning and parsing with and-or graphs," in *Proceedings of the IEEE Conference on Computer Vision and Pattern Recognition*, 2014, pp. 3462–3469.
- [41] Y. Wu, J. Lim, and M.-H. Yang, "Online object tracking: A benchmark," in *Proceedings of the IEEE conference on computer vision and pattern recognition*, 2013, pp. 2411–2418.
- [42] F. Li, C. Tian, W. Zuo, L. Zhang, and M.-H. Yang, "Learning spatial-temporal regularized correlation filters for visual tracking," in *Proceedings of the IEEE conference on computer vision and pattern recognition*, 2018, pp. 4904–4913.
- [43] N. Wang, W. Zhou, Q. Tian, R. Hong, M. Wang, and H. Li, "Multi-cue correlation filters for robust visual tracking," in *Proceedings of the IEEE conference on computer vision and pattern recognition*, 2018, pp. 4844–4853.
- [44] Q. Wang, L. Zhang, L. Bertinetto, W. Hu, and P. H. Torr, "Fast online object tracking and segmentation: A unifying approach," in *Proceedings of the IEEE/CVF conference on Computer Vision and Pattern Recognition*, 2019, pp. 1328–1338.
- [45] D. Guo, J. Wang, Y. Cui, Z. Wang, and S. Chen, "Siamcar: Siamese fully convolutional classification and regression for visual tracking," in *Proceedings of the IEEE/CVF conference on computer vision and pattern recognition*, 2020, pp. 6269–6277.



**Weijie Yan** received his B.S. degree in electronic science and technology from Nanjing University of Science & Technology, Nanjing, China, in 2022. He is currently studying for the M.S. degree in physical electronics from Nanjing University of Science & Technology, Nanjing, China. His main research interests include computer vision, machine learning and image processing.



**Minjie Wan** received his B.S. degree in electronic science and technology from Nanjing University of Science & Technology, Nanjing, China, in 2014 and the Ph.D. degree in optical engineering from Nanjing University of Science & Technology, Nanjing, China, in 2020. He was a visiting Ph.D. student with the Department of Electrical and Computing Engineering, Université Laval, Quebec, Canada, from 2017–2018. He worked as a Post-Doctoral Researcher with the School of Electronic and Optical Engineering, Nanjing University of Science & Technology, from 2020 to 2021, where he is currently an Associate Professor. His main research interests include image processing, computer vision, and computational imaging.



**Yunkai Xu** received his B.S. degree in electronic science and technology from Nanjing University of Science & Technology, Nanjing, China, in 2020. He is currently studying for the Ph.D. degree in optical engineering from Nanjing University of Science & Technology, Nanjing, China. His main research interests include computer vision and machine learning.



**Qian Chen** received the B.S. and M.S. degrees in optoelectronic technology from Nanjing University of Science & Technology, in 1987 and 1991, respectively, and the Ph.D. degree in optical engineering from Nanjing University of Science & Technology, Nanjing, China, in 1996. Since 1996, he has been a Professor with the School of Electronic and Optical Engineering, Nanjing University of Science & Technology, Nanjing, China. His current research interests include optical design and computer version.



**Xiaofang Kong** received the B.S. degree in electronic information engineering and the Ph.D. degree in optical engineering from the Nanjing University of Science & Technology, Nanjing, China, in 2013 and 2020, respectively. She is currently a Post-Doctoral Researcher with the National Key Laboratory of Transient Physics, Nanjing University of Science and Technology. Her research interests include dynamic parameter testing, and photoelectric detection and image processing.



**Guohua Gu** received the B.S. and M.S. degrees in optical instrument from Nanjing University of Science & Technology, Nanjing, China, in 1989 and 1996, respectively, and the Ph.D. degree in optical engineering from Nanjing University of Science & Technology, Nanjing, China, in 2001. Since 2007, he has been a Professor with the School of Electronic and Optical Engineering, Nanjing University of Science & Technology, Nanjing, China. His current research interests include optical design, computer version and machine learning.



**Ajun Shao** received the B.S. degree in electronic science and technology and the M.S. degree in optical engineering from the Nanjing University of Science & Technology, Nanjing, China, in 2012 and 2016, respectively, where he is currently pursuing the Ph.D. degree in optical engineering. His main research interests include infrared imaging and image processing.